Sulistyo SB, Woo WL, Dlay SS.

Regularized Neural Networks Fusion and Genetic Algorithm based On-Field Nitrogen Status Estimation of Wheat Plants.

***IEEE Transactions on Industrial Informatics* (2016)**

DOI: http://dx.doi.org/10.1109/TII.2016.2628439

Regularized Neural Networks Fusion and Genetic Algorithm based On-Field Nitrogen Status Estimation of Wheat Plants

Susanto B. Sulistyo, W.L. Woo, *Senior Member, IEEE*, S.S. Dlay

***Abstract* — The estimation of nutrient content of plants is considerably important in agricultural practices especially in enabling the application of precision farming. A plethora of methods have been used to estimate nitrogen amount in plants, including the utilization of computer vision. However, most of the image-based nitrogen estimation methods are conducted in controlled environments. These methods are not so practical, time consuming and require many equipment. Therefore, there is a crucial need to develop a method to estimate nitrogen content of plants based on leaves images captured on field. It is a very challenging task since the intensity of sunlight is always changing and this leads to an inconsistent image capturing problem. In this research, we develop a low-cost, simple and accurate approach image-based nitrogen amount estimation. Plant images are captured directly under sunlight by using a conventional digital camera and are subject to a variation in lighting conditions. We propose a color constancy method using neural networks fusion and a genetic algorithm to normalize various plant images due to different sunlight intensities. A Macbeth color checker is utilized as the reference to normalize the color of the images. We also develop a combination of neural networks using a committee machine to estimate the nitrogen content in wheat leaves. Twelve statistical RGB color features are used as the input parameters for the nutrient estimation. The obtained result shows considerable better performance than the conventional gray-world and scale-by-max approaches, as well as linear model and single neural network methods. Finally, we show that our nutrient estimation approach is superior to the commonly-used SPAD (soil-plant analysis development) meter based prediction.**

***Index Terms*— computational intelligent image processing, neural networks, committee machines, adaptive learning, color normalization, agriculture engineering**

I. Introduction

RECENTLY, precision farming has become a topical agricultural issue. This concept aims to increase productivity as well as to minimize production costs and negative impacts to environment [1]. The precision farming model, therefore, will lead to a more efficient application with regards to farm resources, such as water, seeds, chemicals and fertilizers. In order to support this idea, it is important to estimate the nutrient status of the plants to improve the efficiency of fertilizer use. Nitrogen (N) is one of the nutrients needed in large amounts by plants to ensure growth. This element is a component of chlorophyll, which has an important function in photosynthesis.

According to [2], there are four common methods utilized to assess nitrogen content in a plant, i.e. chemical and combustion test, normalized difference vegetation index (NDVI), SPAD (soil plant analysis development) meter, and leaf color chart. Nowadays, due to recent developments in computer vision, image-based analysis to estimate nutrient status has been extensively used by numerous researchers due to its rapid and easy data acquisition [3]. This method can be used either to detect nutrient deficiency [4], [5] or to estimate nutrient amount [2], [6]. However, most of the image-based nutrient estimation approaches are conducted in a controlled environment, such as in a closed box with an artificial lighting system [6], [7]. These methods are not so practical, time consuming and require some additional equipment. Such method cannot be applied on-field since the intensity of sunlight is always changing and this will lead to an inconsistent image capturing problem, which motivates the research direction of the present paper. There are a number of challenges in estimating the nutrient content of plants based on images captured on fields, including the effect of various sunlight concentrations, as well as how to normalize images so that all the images captured under both high and low light intensities have small color variability. Note that color images change dynamically with the change of light intensity.

In this paper we develop a low-cost, simple and accurate approach to estimate the nitrogen content in wheat leaves based on leaf images that are captured on-field under sunlight using a conventional digital camera. As seen in Fig. 1, wheat plants from the same field with the same fertilizing level will appear different when the light intensity from the light source is different. Such images cannot be used directly in a nutrient estimation as they are acquired under a different illumination. The images, therefore, need to be normalized so that they can be used for comparison and estimation. After image normalization, the color difference of the wheat leaves is solely caused by the different fertilizing level. In general, the

Accepted on 8th May 2016.

This work was supported by Directorate General of Higher Education Indonesia Ministry of Research and Technology and Jenderal Soedirman University, Purwokerto, Indonesia.

The authors are with the School of Electrical and Electronic Engineering, Newcastle University, England, UK. Correspondence e-mail: w.l.woo@ncl.ac.uk

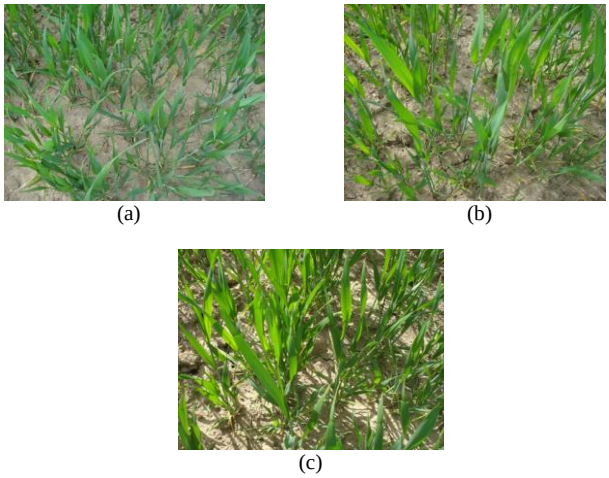

Fig. 1. Examples of wheat plant images captured under different sunlight intensity: (a) low light intensity, (b) medium light intensity, and (c) high light intensity.

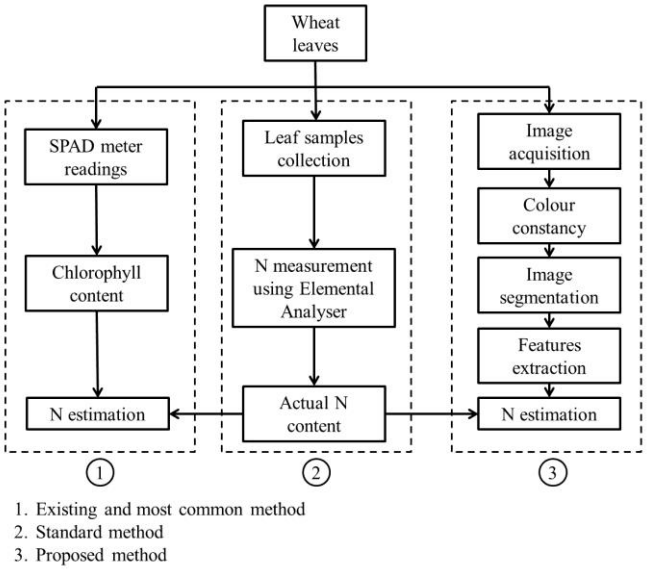

Fig. 2. Flowchart of the whole research.

less nitrogen fertilizer applied to plants, the lighter the green color of the leaves. The next step is image segmentation and features extraction. In this step we apply neural network to distinguish wheat leaves as the object of interest from other images, such as soil, weeds, dried leaves, stems and stones. Twelve statistical features, i.e. first moment (mean), second moment (variance), third moment (skewness) and fourth moment (kurtosis) of each RGB color channel, are extracted from the segmented images as the nutrient estimation predictors. We propose the utilization of these statistical features as predictors, instead of single color channel from certain color model or combination of some color channels, since they signify color distributions in wheat leaves. In the nutrient estimation step, we develop a combination of a committee machine and a genetic algorithm from several neural networks with different hidden layer nodes to estimate nitrogen content.

This paper considers the problem of regularized neural networks fusion and genetic algorithm based on-field nitrogen status estimation of wheat plants. Furthermore, the novel contributions of the proposed approach are concluded below.

1) The problems of color variability due to various light intensities are handled by developing neural networks fusion, which are obtained from 24 color patches of the Macbeth color checker, and its combination with genetic algorithm (GA) for image normalization. In addition, the developed GA is used to determine weights of each neural network.
2) In the nitrogen estimation step, we introduce four statistical features of each RGB color channels which represent the distribution of wheat leaves color as the inputs of the developed neural networks.
3) In order to give the best results of the nitrogen estimation, we develop a committee machine to combine several neural networks and genetic algorithm based optimization to estimate nutrient content.

This paper is organized as follows: experimental set is explained in the next section; the neural networks fusion and genetic algorithm based color constancy for image normalization is discussed in Section III; in Section IV the neural network based image segmentation and statistical color features extraction are described; the nitrogen content prediction using neural networks is explained in Section V; the results of the proposed method are presented and discussed in Section VI; and finally, concludes our research in Section VII.

II. Experimental Setup

This research can be divided into three parts as depicted in Fig. 2. Each part will be explained more detail in the following sections.

A. Experimental Materials and Design

In order to produce variations in nitrogen levels, an experiment in relation to wheat plants with various fertilizer amounts is established. This experiment was conducted at Nafferton experimental farm, Newcastle University, from April to June. The treatments were set to three different fertilizer amounts, i.e. 0 (N1), 85 (N2), 170 (N3) kg/ha of NH_4NO_3 with each treatment replicated four times. Hence, there are 12 plots with each plot being 20 m × 20 m in dimension. The data collection was undertaken in three different sessions i.e. one week prior to fertilizing, and two and four weeks after fertilizing. Therefore, in total 36 samples were used in this research.

B. SPAD meter readings

The SPAD meter readings were conducted on 30 leaf samples in each plot. The value displayed on the SPAD meter screen signified the chlorophyll content of the leaf, which is strongly correlated with the nitrogen content. The SPAD values of the 30 leaves on one plot were then averaged, in order to obtain the SPAD value of the plot. Therefore, there are 12 SPAD values for 12 samples in one data collection time. In total, there are 36 SPAD values used for comparison.

C. Combustion Method based Nitrogen Analysis

The actual nitrogen content is measured using an Elementar Vario Macro Cube. Prior to nutrient analysis, 50-60 leaves per plot were taken as samples. These samples were then dried in a cabinet oven dryer at a temperature of 80^{o}C for 2 days. Subsequently, the dried samples were ground in an electric grinder at 14,000 rpm to pulverize the samples into powder.

For the nitrogen analysis, a sample weight of approximately 100 mg was required, which was weighed into a tin foil cup. The cup was then folded and squashed into a pellet to expel the air. This analysis involved the combustion method by burning the sample with a certain amount of oxygen. The nitrogen element was analyzed and a percentage figure subsequently obtained.

D. Image Acquisition

Under sunlight the crop samples images were indiscriminately captured at 10 points on each plot. Thus, related to image acquisition, we obtained 360 images for 12 plots during three specific times (days). The light intensity of the sun during this experiment ranged from around 8 to 80 Klux with the image data collection time being from 10 am until 2 pm. This means that the color of the sunlight was relatively white, compared to its color in the morning or in the evening, when it is quite reddish or yellowish. All images were captured from the top of the plants in a distance of 10-20 cm using a common digital camera (Sony DSC-W55). The images were recorded at a resolution of 1632 × 1224 pixels and subsequently down sampled to 448 × 336 pixels to assist with the effectiveness of the image processing.

III. Neural Networks Fusion and Genetic Algorithm Based Color Constancy For Image Normalization

The changes in sunlight intensity will lead to different appearances in the plant images. The images, therefore, need to be equalized as if they are acquired under the same light intensity, in order to perform a reliable comparison of the images. In this research, a 24-patch Macbeth color checker has been utilized for the neural network based color constancy to normalize images. The Macbeth color checker is a square card that consists of 24 patches of color samples which represent natural objects, chromatic, primary and grayscale colors, which are arranged in four rows (Fig. 3). Neural networks have been used widely in various industrial applications, such as wind power plants [8], transportation [9], robotics [10], and marine [11]. Neural networks are also used in digital signal processing [12], [13] and electronic applications [14], [15].

Color constancy is an ability to correct the color deviations of an object due to differences in lighting conditions. According to [16], image colors are significantly affected by the direction and intensity of the light source, as well as illuminant color. Furthermore, countless research has been conducted to overcome the problem of color constancy [17]–[19]. In this paper, our color constancy concept differs from previous works given that the images are acquired under unconstrained daylight, as mentioned in Section II.D. This poses a more difficult challenge as plant images captured under various light intensities have to be corrected to a standard image that is captured under a standard light intensity.

Fig. 3. Macbeth color checker.

Our proposed method of neural networks fusion and genetic algorithm for image normalization is described below. First, the image of the Macbeth color checker is captured under sunlight using the digital camera and subject to variations in light intensity. The measured light intensity had a range of 7 to 82 Klux. The 50 Klux is considered to be the standard (target) light intensity and the remainder as the input light intensity. In total there are 164 input images (range of 7 to 48 Klux and 52 to 82 Klux) and five target images (range of 49-51 Klux). Each image is consequently cropped twice on each patch with a cropping size of 95 × 72 pixels. The average RGB color value of each patch of the cropped input images is then calculated. The average RGB value of each patch of the target images is obtained from five images. Thus, we have 24 datasets of input-target RGB color from 24 patches and with each patch consisting of 328 (= 164 × 2) RGB color samples.

All the datasets are consequently combined to produce one large dataset for neural networks fusion. This new dataset, thus, consists of 7872 (= 328 × 24) RGB color samples. The single neural network for each color patch developed in this research is a multilayer perceptron (MLP), which contains one hidden layer, three nodes of input and output layers of red, green and blue color channels. MLP is a well-established neural network that can be used for classifier [20] as well as nonlinear model prediction [21]. The cost function is based on minimizing the mean square error (MSE) between the targets and the outputs of the MLP. The number of hidden layer nodes in each network is determined by applying the formula developed by [22] as follows:

$$n_h = \left(\frac{n_i+n_o}{2}\right) + \sqrt{n_p} \quad (1)$$

where n_i, n_h and n_o are the number of input, hidden and output layer nodes, respectively, and n_p is the number of input patterns in the training set (number of training samples).

According to Eq. (1), the number of hidden layer nodes for each neural network is 92 nodes ($n_i = 3$,$n_o = 3$, $n_p = 7872$). However, we found that this method serves only as a guide and does not always provide the optimal number of hidden nodes. In this paper, we propose a new method that optimizes the MSE and imposes a smooth regularization on the weights of the hidden nodes in addition to implementing (1). To this end, we focus on the following smoothness function [15]:

$$\Omega = \frac{1}{2}\int \Upsilon(\boldsymbol{X})\left\|\partial^k G(\boldsymbol{X})/\partial \boldsymbol{X}^k\right\|\boldsymbol{X}\,\partial \boldsymbol{X} \quad (2)$$

develop the weighting function $\Upsilon(\boldsymbol{X})$ that ensures the above integral converges and subsequently determines the region of the input space over which the MLP mapping $G(\boldsymbol{X})$ is required to be smooth by making the k^{th} order derivative of $G(\boldsymbol{X})$ with respect to input $\boldsymbol{X}$ small. The larger the value of k, the smoother the mapping $G(\boldsymbol{X})$ will become. We propose the following mixture of Gaussian functions:

$$\Upsilon(\boldsymbol{X}) = \frac{1}{Q}\sum_{k=1}^{Q}\frac{1}{(2\pi)^{N/2}|\boldsymbol{R}|^{1/2}}\exp\left[-\frac{1}{2}(\boldsymbol{X}-\boldsymbol{X}_k)^T\boldsymbol{R}^{-1}(\boldsymbol{X}-\boldsymbol{X}_k)\right] \quad (3)$$

so as to capture the local variation of the input space where $\{\boldsymbol{X}_k\}_{k=1}^{Q}$ are a set of input data points and that using $\boldsymbol{R} = \sigma^2\mathbf{I}$, it is required that σ be selected small such that

$$\lim_{\sigma\to\infty}\sum_{k=1}^{Q}\frac{1}{(2\pi\sigma^2)^{N/2}}\exp\left[-\frac{1}{2\sigma^2}\|\boldsymbol{X}-\boldsymbol{X}_k\|^2\right] = \delta(\boldsymbol{X}-\boldsymbol{X}_k) \quad (4)$$

where $\delta(\cdot)$ is the delta function. The above integral can be approximated as

$$\Omega \approx \frac{1}{2}\sum_{j,k} w_{jk}^2\|\boldsymbol{v}_k\|^p \quad (5)$$

where $\boldsymbol{v}_k = [v_{k1} \quad v_{k2} \quad \cdots \quad v_{kn_h}]$ is the k-th row of weight matrix $\boldsymbol{V}$ connecting the input to the hidden nodes, $\|\cdot\|^p$ is the p-norm. The simple algebraic form of Ω enables the direct enforcement of smoothness without the need for costly Monte-Carlo integrations. The derivatives of the weighting function Ω with respect to the parameters w_{jk} and v_{ij} have been derived as follows:

$$\frac{\partial\Omega}{\partial w_{jk}} = w_{jk}\|\boldsymbol{v}_k\|^p \quad (6)$$

and

$$\frac{\partial\Omega}{\partial \boldsymbol{v}_k} = \frac{p}{2}(\boldsymbol{v}_k)^{p-1}\sum_j w_{jk}^2 \quad (7)$$

The steps taken in the MLP neural network can be described as follows:

1. Normalize inputs (X_i)
   RGB input colors should be normalized by dividing their values with the maximum value 255. Thus, $X_1 = \frac{\mathrm{R}}{255}, X_2 = \frac{\mathrm{G}}{255}, X_3 = \frac{\mathrm{B}}{255}$; $X_i \in [0,1],\ i = 1,2,3$.
2. Initialise all weights (v_{ij} and w_{jk})
   Set weights related to hidden and output layers to small random values (between -1 to 1). Thus $v_{ij},\ w_{jk} \in [-1,1]$, $i,k = 1,2,3;\ j = 1,2,3,\ldots,n_h$ where n_h is the number of hidden unit.
3. Calculate activation function (forward propagation)
   In the multilayer perceptron neural networks, outputs of one layer become inputs of the next layer.

$$Z_j = f^{(1)}\left(\theta_j^{(1)} + \sum_{i=1}^{3} X_i v_{ij}\right) \quad (8)$$

$$Y_k = f^{(2)}\left(\theta_k^{(2)} + \sum_{j=1}^{p} Z_j w_{jk}\right) \quad (9)$$

   where $\theta_j^{(1)}$ is the bias on hidden unit j and $\theta_k^{(2)}$ is the bias on output unit k, Z_j is the output of hidden unit j, and Y_k is the output of output unit k. In this research, we use sigmoid activation function with regards to the hidden layer ($f^{(1)}$) and linear function for the output layer ($f^{(2)}$) to gain the output signal for each layer.
4. Calculate the networks error (backward propagation)

$$\delta_k^{(2)} = (T_k - Y_k)f'^{(2)}\left(\theta_k^{(2)} + \sum_{j=1}^{p} Z_j w_{jk}\right) \quad (10)$$

$$\delta_j^{(1)} = \left(\sum_{k=1}^{3}\delta_k^{(2)} w_{jk}\right)f'^{(1)}\left(\theta_j^{(1)} + \sum_{i=1}^{3} X_i v_{ij}\right) \quad (11)$$

   where T_k is the target of unit k, $\delta_k^{(2)}$ is error correction for output layer weights and $\delta_j^{(1)}$ is error correction for hidden layer weights.
5. Update all weights and biases
   Compute weights and biases of n-th iteration using the following formulae:

$$w_{jk}(n) = w_{jk}(n-1) + \eta_1\left(\delta_k^{(2)} Z_j + \eta_2 w_{jk}\|\boldsymbol{v}_k\|^p\right) \quad (12)$$

$$v_{ij}(n) = v_{ij}(n-1) + \eta_1\left(\delta_j^{(1)} X_i + \eta_2\frac{p}{2}(\boldsymbol{v}_k)^{p-1}\sum_j w_{jk}^2\right) \quad (13)$$

$$\theta_k^{(2)}(n) = \theta_k^{(2)}(n-1) + \eta_1\left(\delta_k^{(2)} + \eta_2 w_{jk}\|\boldsymbol{v}_k\|^p\right) \quad (14)$$

$$\theta_j^{(1)}(n) = \theta_j^{(1)}(n-1) + \eta_1\left(\delta_j^{(1)} + \eta_2\frac{p}{2}(\boldsymbol{v}_k)^{p-1}\sum_j w_{jk}^2\right) \quad (15)$$

   where η_1 is a fixed learning rate while $\eta_2 = 1/n$ is a adaptive learning rate that reduces exponentially. The stability of the neural network weights update equations can be analyzed by utilizing the mean-value theorem and introducing the Nussbaum function as proposed in [23], [24].
6. Repeating the cycle.
   The above processes (no. 3–5) are repeated until one of the following conditions is reached:
   a. The maximum number of iteration is reached.
   b. The maximum amount of time has been exceeded.
   c. Performance error is less than the goal set.
   d. The performance gradient falls below the minimum performance gradient.

The next step is combining all the single networks into one neural network system. The proposed neural networks fusion, as observed in Fig. 4, is developed to generate new RGB outputs. The final output RGB values from the networks fusion is obtained as follows:

$$\begin{aligned}\mathbf{Z} &= \boldsymbol{\alpha}\cdot\mathbf{O}\\ &= [\propto_1, \propto_2, \propto_3, \cdots, \propto_{24}]\cdot[\boldsymbol{O}_1, \boldsymbol{O}_2, \boldsymbol{O}_3, \cdots, \boldsymbol{O}_{24}]^T\end{aligned} \quad (16)$$

where $\boldsymbol{\alpha}$ is the weight matrix of each network output, $\mathbf{O}$ is the output matrix of each neural network and $\mathbf{Z}$ is the final output

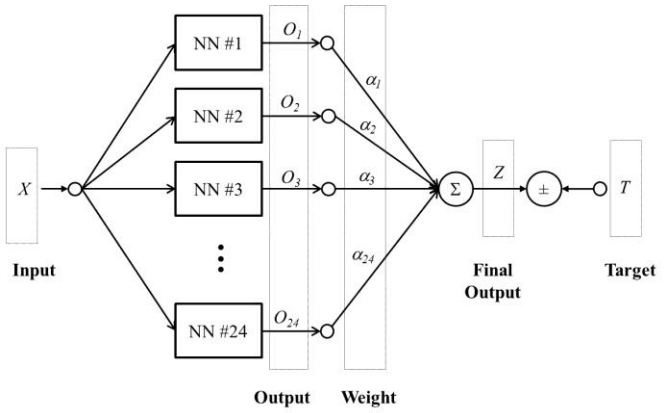

Fig. 4. The proposed neural networks fusion using Macbeth color checker.

matrix of the neural networks fusion. From the Eq. (16), it can be distinguished that matrix $\boldsymbol{\alpha}$ consists of 24 diagonal α matrices with dimension of 3 × 3. Similar to matrix $\boldsymbol{\alpha}$, matrix $\mathbf{O}$ also has 24 matrices with a dimension of 3 × N for each matrix $\boldsymbol{O}_i$, whilst N is the number of training samples.

In this paper, a genetic algorithm is utilized to find the optimum value for each of the 24 $\boldsymbol{\alpha}$ matrices. Genetic algorithm (GA) is an algorithm based on the Darwin principle of evolution, natural selection and biological systems. It has been extensively used for optimization in many fields, for instance, plug-in hybrid electric vehicles' (PHEVs) integration [25], plastic film manufacturing process [26], automatic path planning of unmanned aerial vehicles [27], and design of photovoltaic systems [28]. Basically, genetic algorithm encompasses a population with a certain number of individuals. Each individual in a population has the possibility of being the solution to the optimization problem. Hence, by applying crossing over and mutation among individuals, a new generation is produced. This process is repeated several times until a new individual provides the most appropriate solution for the problem.

In this research, several methods have been conducted to determine the optimum $\boldsymbol{\alpha}$. In our experiments, the developed neural networks fusion can be optimized by using a genetic algorithm with the following conditions:

1. Initial population size is 1,000 individuals.
2. The $\boldsymbol{\alpha} = [\propto_1, \propto_2, \propto_3, \cdots, \propto_{24}]$ matrix has a dimension of 3 × 72 and every element of matrix $\propto_k$ is expressed by a 10-bit string of binary number (0s and 1s).
3. Permutation rate is 0.75.
4. The boundary of each element with regards to each matrix $\propto_k$, i.e. $a_{k,ij}$ with $i, j = 1, 2, 3$, is set as follows:
   if $i = j$ then $a_{k,ij} \in [0, 0.1]$
   else $a_{k,ij} = 0$

   Thus, each matrix α_k is constructed as follows:

$$\alpha_k = \begin{bmatrix} a_{k,11} & 0 & 0 \\ 0 & a_{k,22} & 0 \\ 0 & 0 & a_{k,33} \end{bmatrix} \quad (17)$$

   with $k = 1, 2, 3, \ldots, 24$.
5. The fitness function is based on the mean square error between the target and the final output RGB values.

The steps of the developed genetic algorithm for training the matrix $\boldsymbol{\alpha}$ can be described as follows:

1. Generate the initial population, i.e. 1000 individuals, with 2,160 (= 10 × 3 × 72) bits length for each individual.
2. Produce the next generation by processing cross-over and mutation on each individual.
3. Compute the fitness for each individual.
4. Select the best individual with *MSE* lower than 0.0001.

Once the optimum value of matrix $\boldsymbol{\alpha}$ is achieved, the next step is applying the developed neural networks fusion and matrix $\boldsymbol{\alpha}$ to adjust the RGB color of the wheat plants. In this research, a wheat plant image has a dimension of 448 × 336 pixels. Through this developed color adjusting system, each pixel of a plant image acquired under various light intensities is transformed to the equivalent pixel of the image under the standard light intensity, i.e. 50 Klux.

IV. Neural Network Based Image Segmentation and Statistical Color Features Extraction

Image segmentation plays an important role in classifying each pixel in an image either as a targeted object or a background part. For instance, in controlled image capturing circumstances, an object is laid down on a white paper background in a closed box with certain illuminations; the object in the captured image can easily be distinguished from its background by applying a simple threshold value. In this research, however, the problem is more complicated. The images of the wheat leaves are captured directly in the field and contain leaves as the targeted object, in addition to other unwanted parts, such as soil, stones, weeds, and dried and semi-dried leaves in the background. Many of the unwanted parts (especially the weeds and semi-dried leaves) have a similar color to the wheat plant.

A multilayer, feed forward, back-propagation error neural network is used for image segmentation to distinguish the wheat leaves, as the region of interest, from other undesired parts. The developed neural network for this step can be explained as follows:

1. The network has three units of input layer, which indicate red, green and blue color values (RGB) for each pixel related to the plant images with a range of 0 – 255.
2. The number of hidden units is 30.
3. The output layer has only one unit, which signifies whether each pixel is a part of a leaf or not. The output value of the network is equal to 1 if the corresponding pixel is a part of a leaf, otherwise the value is 0.
4. The sigmoid activation function is used for both hidden and output layers.
5. The step size η_1 is set to be a small constant. When η_1 is large, the convergence of the neural network parameters will be quicker than that when η_1 is small. However, large η_1 leads to larger fluctuation around the steady state mean square error. On the other hand, small η_1 leads to smaller fluctuation around the steady state mean square error but the convergence rate of the neural network parameters is

low. Thus, there is a trade-off between accuracy and speed of convergence. In our case, we have experimented with various settings of η_1 and we find that $\eta_1 = 0.0025$ leads to the best performance. As for η_2, this is set according to the decay process i.e. $\eta_2 = 0.05/n$ where n is the iteration number. In this way, the smoothness regularization has more impact on the neural network parameters at the start of the learning process but slowly tapers off after some time to allow convergence to the desired solution.

For the developed neural network, we have a dataset of 4,800 samples of RGB color and binary values (0 or 1) as the input and target values, respectively. The dataset was achieved from 24 images. On each image, 100 pixels in the leaf region and 100 pixels in other parts of the region were selected manually. The RGB color values of the selected pixels were then used as inputs of the network.

In the color segmented image, noise should be removed prior to the features extraction step. In the majority of images, weeds are also present which need to be eliminated from the segmented image, as they can influence the color information of the wheat leaves. To resolve this problem, we use the largest part of the leaves which has the highest number of object pixels. This algorithm can be seen in Fig. 5. An example of the results of image normalization using neural networks fusion and image segmentation can be seen in Fig. 6. As revealed, the proposed color constancy method for image normalization and the neural networks based image segmentation can be used in an automated manner to normalize the images of the plants and to remove the unwanted parts from the image, as indicated by the black circles.

In the features extraction step, several statistical color features pertaining to the final color segmented images are calculated. These features are used for nutrient estimation in the next step. Four statistical features are used in this research, i.e. first raw moment (mean), second central moment (variance), third central moment (skewness) and fourth central moment (kurtosis). Thus, there are 12 statistical features for all color channels (red, green and blue). These features represent the color distributions related to the segmented images, whilst the mean is considered to be the central tendency of the color distribution. The variance measures the spread of color distribution from the mean; whereas skewness determines the symmetricity of color distribution and kurtosis measures the ridge color distribution. In addition, color moments have been extensively and successfully used in color-based image retrieval systems, especially for a segmented image which contains only the image of object [~~27~~ 29]. The statistical color features can be achieved by using the following formulae:

$$mean = \bar{y} = \frac{1}{n}\sum_{i=1}^{n} y_i \tag{18}$$

$$variance = \sigma^2 = \frac{1}{n}\sum_{i=1}^{n}(y_i - \bar{y})^2 \tag{19}$$

$$skewness = skew = \frac{\frac{1}{n}\sum_{i=1}^{n}(y_i - \bar{y})^3}{\sigma^3} \tag{20}$$

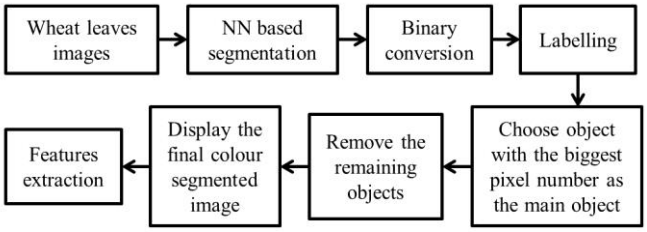

Fig. 5. Image segmentation algorithm.

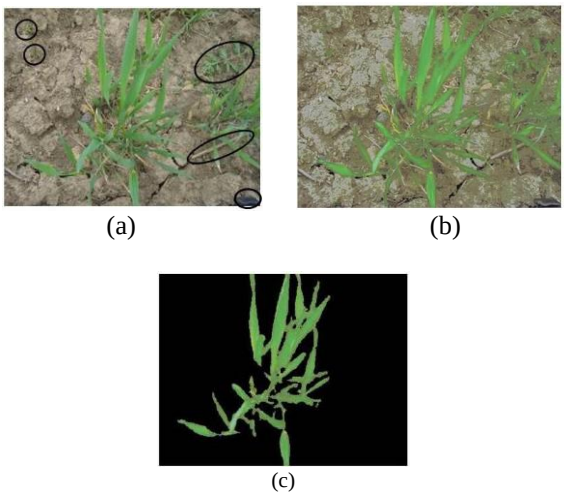

Fig. 6. An example of the results of BPNN based color constancy and image segmentation; (a) original image, (b) normalized image, (c) segmented image.

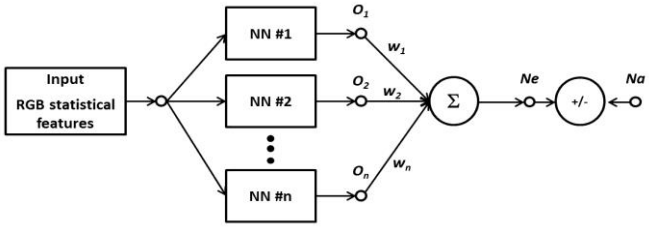

Fig. 7. Combination of neural networks for nitrogen estimation.

$$kurtosis = kurt = \frac{\frac{1}{n}\sum_{i=1}^{n}(y_i - \bar{y})^4}{\sigma^4} \tag{21}$$

where y refers to each color channel (red, green and blue), n is the number of object pixels and σ is the standard deviation.

V. Nitrogen Content Estimation Using Weighted Neural Networks

In this section, we will describe the final step of our proposed method, i.e. nitrogen estimation. An MLP with back propagation error is used to determine the nitrogen amount in wheat leaves. The developed neural network consists of 12 nodes of input layer which corresponds to the statistical color features and one node of output layer that corresponds to the percentage related to the nitrogen amount. In this step, the number of hidden layer nodes is also determined by using Eq. (1). Twelve hidden nodes are subsequently obtained according to 12 input features, one output unit and 36 input samples.

In this paper, we also employ committee machines to

combine several neural networks with different hidden layer nodes, as seen in Fig. 7. The numbers of hidden layer nodes with regards to these new neural networks are produced using the following formula:

$$n_h' = s \times n_h \tag{22}$$

where n_h' is the new number of hidden layer nodes, n_h is the initial number of hidden layer nodes (i.e. 12 nodes) and s is the multiplication factor (s = 2, 3, …, n), whilst n is the number of combined neural networks (in this paper we attempted up to 7 neural networks).

In this case, the parameter s is also the number of neural networks used for the combination. Thus, the networks combinations attempted in this step are as illustrated in Table I. Each network is repeated 100 times to eliminate the effect of the random bias numbers and initial weights. Subsequently, a number of neural networks which provided the minimum mean square error are chosen to achieve the final estimation.

A committee machine can produce significant improvements in the prediction given that it can minimize the effect of a random component due to data noise in the generalization performance of a single network [30, 31]. Basically, the concept of a committee machine is to combine outputs of several expert systems with the same input data, with the aim of producing a new output. In this paper, we use ensemble averaging as the combination method. Suppose that there are *P* expert systems to approximate a target vector *T*. Each expert has output vector O_i and error e_i,

$$O_i = T + e_i \tag{23}$$

Thus, the sum of the squared error for the *i*-th expert y_i is

$$E_i = \xi[(O_i - T)^2] = \xi[e_i^2] \tag{24}$$

where $\xi[\cdot]$ denotes the statistical expectation.
The average error of each expert system (E_{ave}) is then

$$E_{ave} = \frac{1}{P}\sum_{i=1}^{P} E_i = \frac{1}{P}\sum_{i=1}^{P} \xi[e_i^2] \tag{25}$$

In other words, by using a committee machine, the output value *Y* can be achieved by simply averaging the output vector O_i, as follows:

$$Y = \frac{1}{P}\sum_{i=1}^{P} O_i \tag{26}$$

Thus, the squared error of the committee machine (E_{COM}) is

$$\begin{aligned} E_{COM} &= \xi[(Y - T)^2] \\ &= \xi\left[\left(\frac{1}{P}\sum_{i=1}^{P} O_i - T\right)^2\right] = \xi\left[\left(\frac{1}{P}\sum_{i=1}^{P} e_i\right)^2\right] \end{aligned} \tag{27}$$

But

TABLE I
NEURAL NETWORKS COMBINATION

Number of NNs	Number of hidden layer nodes
2	12 – 24
3	12 – 24 – 36
4	12 – 24 – 36 – 48
5	12 – 24 – 36 – 48 – 60
6	12 – 24 – 36 – 48 – 60 – 72
7	12 – 24 – 36 – 48 – 60 – 72 – 84

$$\xi\left[\left(\frac{1}{P}\sum_{i=1}^{P} e_i\right)^2\right] \le \frac{1}{P}\sum_{i=1}^{P} \xi[e_i^2]$$

Thus, we have

$$E_{COM} \le E_{ave} \tag{28}$$

The calculated error of the committee machine is always smaller than if not equal to that of the single expert. In this paper, we use ensemble averaging as the neural networks combiner to obtain improved generalization and performance. The estimated nitrogen amount of wheat leaves is calculated by using a committee machine with the simple averaging method as the combiner of *n* neural networks, as follows:

$$Ne_{ave} = \frac{1}{n}\sum_{i=1}^{n} O_i \tag{29}$$

The simple averaging method as expressed in Eq. (29) indicates that each single neural network has the same weight to produce the new output. In this paper, we also investigate the possibility that each neural network has a different weight. We apply a weighted averaging method, as expressed in the following:

$$Ne_{weigh} = \sum_{i=1}^{n}(w_i \times O_i) \text{ and } \sum_{i=1}^{n} w_i = 1 \tag{30}$$

where Ne_{weigh} is the estimated nitrogen content, w is the weight, and O_i is the output of *i*-th single network.

A genetic algorithm is used to discover the optimum value of the weights in the developed committee machine. The genetic algorithm for the nitrogen estimation is developed with the following conditions:

1. Initial population size is 500
2. Each individual is expressed by 16 (= 2 × 8) bits length of binary numbers
3. Permutation rate is 0.5
4. Each weight has a range of 0–1; $w_i \in [0, 1]$
5. The fitness function is to estimate the mean square error (*MSE*) between the actual and the estimated nitrogen content.

The level of the prediction accuracy is measured by calculating the error value of the observed/actual and predicted nitrogen content. In this research, we use the mean absolute percentage error (*MAPE*) for the performance assessment. The less the error is, the superior the prediction is. For a comparison, several types of error are also measured, i.e. mean absolute error (*MAE*), mean of squared error (*MSE*), root

mean of squared error (*RMSE*) and sum of squared error (*SSE*). The error types used in this research can be expressed as follows:

$$MAPE = \frac{100\%}{n}\sum_{i=1}^{n}\left|\frac{Na_i - Ne_i}{Na_i}\right| \quad (31)$$

$$MAE = \frac{1}{n}\sum_{i=1}^{n}|Na_i - Ne_i| \quad (32)$$

$$MSE = \frac{1}{n}\sum_{i=1}^{n}(Na_i - Ne_i)^2 \quad (33)$$

$$RMSE = \sqrt{\frac{1}{n}\sum_{i=1}^{n}(Na_i - Ne_i)^2} \quad (34)$$

$$SSE = \sum_{i=1}^{n}(Na_i - Ne_i)^2 \quad (35)$$

where n is the number of samples, Na and Ne are the actual and the estimated (using either simple (29) or weighted average (30)) nitrogen content, respectively.

VI. Results and Discussions

A. SPAD meter based nitrogen amount prediction

The SPAD meter was widely used to determine the chlorophyll content in the leaves by measuring the absorbance of the leaf in two wavelength regions, i.e. red and infrared. After the signal processing steps, the absorbance was displayed in a units range from 0 to 199. Moreover, the chlorophyll amount was highly correlated with the nitrogen content. Furthermore, the chlorophyll content which is represented by the SPAD value, increased in proportion to the nitrogen amount.

Based on our experiments conducted with 36 samples of wheat leaves, the coefficient of determination (R^2) value of SPAD readings and nitrogen content is 0.7801, as seen in Fig. 8. It means that the relationship between the SPAD and nitrogen amount was reasonably strong. By using the trend line equation, the predicted nitrogen level was calculated. The *MAPE* of this prediction was 8.48%. Fig. 9 demonstrates the fitting plot between the actual and predicted nitrogen content. Similar research with relatively strong relationships between the SPAD and nitrogen have been reported in sugarcane (R^2 = 0.706) [2] and oilseed rape (R^2 = 0.744) [32]. The correlation between the SPAD meter readings and nitrogen percentage in leaves was strongly affected by leaf thickness. The variation in leaf thickness can influence the accuracy of SPAD meter readings, as this device works based on the leaf's capacity to absorb red and infrared lights.

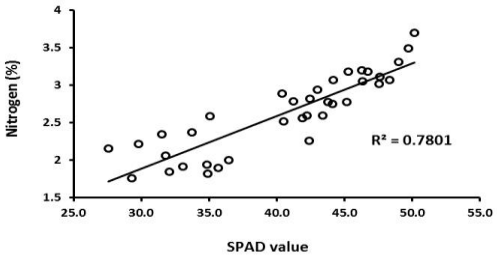

Fig. 8. Relationship between the SPAD value and actual nitrogen content.

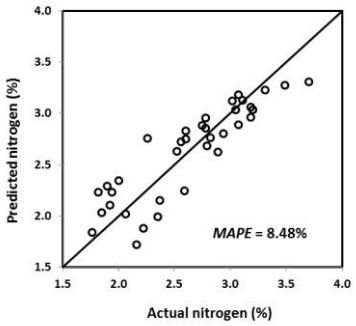

Fig. 9. Fitting plot of the actual and predicted nitrogen content of SPAD meter based prediction.

B. Image-based nitrogen amount prediction

The proposed neural networks fusion based color constancy can be used to normalize plant images captured under various light intensities. After image normalization, we can assume that all images are captured under the same light intensity and compared with each other.

In the color constancy step, we also compare our results with other methods, i.e. gray world and scale-by-max algorithms, linear model, and one single neural network (NN) [33]. The gray world (GW) and scale-by-max (SBM) approaches are the simplest color constancy algorithms due to their ease and simplicity of application. In the gray world algorithm, the average of all colors in an image is considered to be neutral gray. This algorithm yields illuminant estimation by calculating the mean value of each color channel. Hence, to normalize an image, the color value of each pixel is scaled by

$$K_{GW}^{i} = \frac{C}{C_{avg}^{i}} \quad (36)$$

with

$$C = mean\left(C_{avg}^{1}, C_{avg}^{2}, C_{avg}^{3}\right) \quad (37)$$

where i refers to each color channel (red, green and blue).

In the scale-by-max approach, the illuminant estimation is acquired by determining the maximum response of each color channel. Hence, the color value of each pixel can be normalized by multiplying it with the following constant:

$$K_{SBM}^{i} = \frac{255}{\max(i)} \quad (38)$$

In the linear model, the color values of each pixel are corrected through a transformation matrix [34]. Suppose that under an unknown lighting condition, with the transformation matrix M_{un}, the color values of an object q_{un} is as follows:

$$q_{un} = M_{un} r \quad (39)$$

$$r = M_{un}^{-1} q_{un} \quad (40)$$

where r is three basic functions related to surface reflectance. The color values of the standard illumination q_{st}, i.e. in this

research, the light intensity of 50 Klux can be calculated as

$$q_{st} = M_{st} r = M_{st} M_{un}^{-1} q_{un} = M_{tr} q_{un} \quad (41)$$

$$M_{tr} = q_{un}^{-1} q_{st} \quad (42)$$

where M_{tr} is the 3 × 3 transformation matrix. Basically, the NN and the proposed methods discussed in the present paper can be seen as a nonlinear extension of (41). The nonlinear model used in this paper is determined by calculating the transformation in (42) using the back-propagation neural network algorithm, consequently the M_{tr} is used to correct plant images. Alternative types of neural network that have specific structure in the form of $q_{st} = f(M_{tr} f^{-1}(q_{un}))$ which is the nonlinear version of (41) can be devised as in [13, 37-40].

In this paper, we establish that our proposed method is better than the other methods that have previously been mentioned, as seen in Table II. As the basis for the comparison, we measure color differences by calculating the mean Euclidean distance of the targeted and the output (estimated) color value of each method. The formula for the Euclidean distance can be written as follows:

$$\Delta E_{RGB} = \sqrt{(R_t - R_e)^2 + (G_t - G_e)^2 + (B_t - B_e)^2} \quad (43)$$

In our proposed method, by using a 24-patch Macbeth color checker as the reference, we obtain 24 α values as output weights for each neural network. These α matrices are then applied to correct wheat plant images by using the developed neural networks fusion method. An example of the α matrices used to produce a new output is as follows:

$$Z = \begin{bmatrix} 0.087 & 0 & 0 \\ 0 & 0.076 & 0 \\ 0 & 0 & 0.005 \end{bmatrix} \cdot O_1 + \begin{bmatrix} 0.087 & 0 & 0 \\ 0 & 0.027 & 0 \\ 0 & 0 & 0.090 \end{bmatrix} \cdot O_2 + \begin{bmatrix} 0.033 & 0 & 0 \\ 0 & 0.071 & 0 \\ 0 & 0 & 0.099 \end{bmatrix} \cdot O_3 + \cdots + \begin{bmatrix} 0.026 & 0 & 0 \\ 0 & 0.001 & 0 \\ 0 & 0 & 0.019 \end{bmatrix} \cdot O_{24}.$$

In this research, a wheat plant image has a dimension of 448 × 336 pixels. By applying this developed color adjusting system, each pixel of a plant image captured under various light intensities will be transformed to the equivalent pixel of the image under the standard light intensity, i.e. 50 Klux. In order to demonstrate the effectiveness of the proposed method, 30 plants images which are from the same treatment of fertilizer dosage have been selected. Since the images are subject to the same treatment, they should have similar color or, in other words, the color variability should be small. As the focus of the whole research is on the color of the leaves, the original and the corrected images are then segmented to obtain the leaves images as the region of interest. In the segmented images, our proposed color normalization can be used to reduce the variability of leaves color which can be expressed in the standard deviation values. The standard deviations of the original leaves images are 24.76, 16.45 and 30.39 for red, green and blue color respectively, whilst the standard deviation RGB color values of the corrected images are 6.38, 4.07 and 7.58, respectively. This shows that the proposed method has successfully reduced the color variability in the images by approximately four times.

TABLE II
COMPARISON OF COLOR CONSTANCY RESULTS

Methods	ΔE_{RGB}
Gray world	23.40
Scale-by-max	14.86
Linear model	11.06
Single neural network (NN)	5.03
The proposed method (NN fusion)	4.15

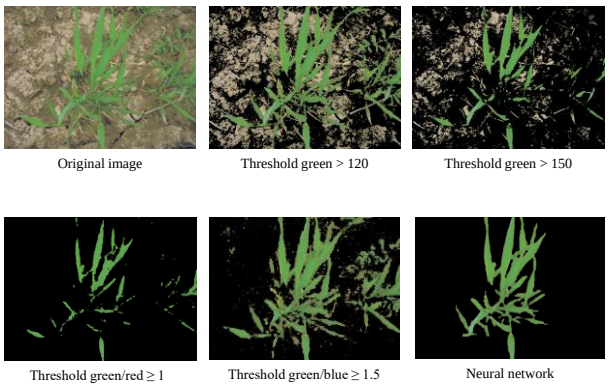

Fig. 10. A comparison of some threshold based and the developed neural network based image segmentations.

After image correction using the developed neural networks fusion, the next step is image segmentation. The neural network based image segmentation, as described in Section IV, can be applied to distinguish wheat leaves from other parts, such as weeds, soil, stones and dried leaves. This segmentation method is superior to the conventional Otsu algorithm (threshold-based segmentation). The database pertaining to the color of leaves and non-leaves provides sufficient data to train the plant images. Therefore, the neural network can precisely classify whether a pixel belongs to the leaves or non-leaves region. A comparison of image segmentation results using Otsu algorithm and the developed neural network can be seen in Fig. 10.

Once all images have been segmented, 12 statistical color features as described in Section IV are subsequently extracted. These features are then utilized as predictors in the developed nitrogen estimation. In this step, several neural networks with different numbers of hidden layer nodes are combined, as tabulated previously in Table I. These combinations of networks are subsequently trained to determine which offers the most appropriate results. After conducting Monte-Carlo testing of more than 100 independent trials, we establish that the combination of six neural networks results in the minimum generalization error of networks performance compared to other possible combinations. The first combination used in this step is a simple average. The estimated nitrogen amount is then calculated, as follows:

$$Ne_{ave} = \frac{1}{6}\sum_{i=1}^{6} \boldsymbol{O}_i \quad (44)$$

The best result relates to the first type of committee machine, i.e. simple average, is subsequently compared to that of the second type combiner, i.e. weighted average, which is optimized by the genetic algorithm (GA). By using this method, the weights of the output of the networks are 0.008, 0.091, 0.140, 0.219, 0.047 and 0.495 respectively for the first until the sixth neural network. The estimated nitrogen content can therefore be expressed as follows:

$$Ne_{GA} = (0.008 \times \boldsymbol{O}_1) + (0.091 \times \boldsymbol{O}_2) + (0.140 \times \boldsymbol{O}_3) + (0.219 \times \boldsymbol{O}_4) + (0.047 \times \boldsymbol{O}_5) + (0.495 \times \boldsymbol{O}_6) \quad (45)$$

Table III illustrates the comparison of various types of error values of the discussed NN and SPAD meter methods. From that table, we can perceive that by using a simple average combiner, the combination of six neural networks provides the best results compared to other network combinations. In addition, the MAPE of this combination is less than 3%. However, the weighted average combiner with GA optimization offers enhanced results. As seen in the table, the MAPE of the GA-based committee machine with six neural networks is smaller than the simple average method, i.e. 2.73%. In other words, the deviation of the estimated nitrogen using this method is approximately 2.73% of the true nitrogen percentage. For instance, if the actual nitrogen content is 3%, then the estimated nitrogen is between 2.92% and 3.08%. Thus, the error noted is relatively small.

In this research, we also investigated the relationship between nitrogen content and each color channel in addition to a number of combinations of them. Research has established that there are significant correlations between chlorophyll content in the maize leaf and the averages of the R and G components, as well as 2G-R-B of the linear transformation [6]. We also estimated the nitrogen content using the greenness index developed by [35] (I_{kaw}). I_{kaw} is defined as follows:

$$I_{kaw} = \frac{R-B}{R+B} \quad (46)$$

Based on the I_{kaw} formula, [36] modified the greenness index to estimate nitrogen content in barley leaves and use the principal component analysis (PCA) to produce a new greenness index (I_{PCA}), as follows:

$$I_{PCA} = 0.7582|R-B| - 0.1168|R-G| + 0.6414|G-B| \quad (47)$$

According to our investigation, single color features and their combinations, including I_{PCA} and I_{kaw}, are not suitable for nitrogen estimation. The estimation errors of those analyses are too high, compared to our proposed method, as seen in Table IV. The RGB values in those analyses are only obtained from the mean value of the observed leaves color. This value is not sufficient to represent the color distribution of leaves color. In the proposed method, we utilize not only mean value, but also variance, skewness and kurtosis of the observed leaves color. The use of these statistical features is more effective to describe the color distribution of leaves color. As seen in the table our proposed method is superior to all the discussed methods, as it provides an estimation error of 2.73%.

TABLE III
COMPARISON OF NITROGEN AMOUNT ESTIMATION ERRORS

Methods	MAPE	MAE	MSE	RMSE	SSE
SPAD meter	8.48%	0.2042	0.0578	0.2404	1.5704
Simple averaged 2 NNs	3.68%	0.0907	0.0150	0.1224	0.5395
Simple averaged 3 NNs	3.12%	0.0780	0.0106	0.1030	0.3821
Simple averaged 4 NNs	3.04%	0.0761	0.0100	0.0999	0.3591
Simple averaged 5 NNs	3.12%	0.0774	0.0102	0.1010	0.3675
Simple averaged 6 NNs	2.93%	0.0731	0.0093	0.0967	0.3363
Simple averaged 7 NNs	3.00%	0.0757	0.0096	0.0979	0.3451
GA averaged 6 NNs	2.73%	0.0674	0.0078	0.0885	0.2819

TABLE IV
COMPARISON OF ESTIMATION ERRORS USING COLOR FEATURES AND THE PROPOSED METHOD

Features	R	G	B	G/R	G/B
MAPE (%)	10.49	13.72	15.87	11.21	12.15
Features	G-R	2G-R-B	I_{kaw}	I_{PCA}	Proposed method
MAPE (%)	12.10	16.56	9.84	9.20	2.73

VII. CONCLUSION

A low cost, simple and accurate nitrogen estimation of wheat leaves has been conducted using the proposed method. The proposed method focuses on color constancy to normalize plant images that are subject to a variation in lighting conditions, besides the application of back-propagation neural network for image segmentation and committee machines for nitrogen content estimation. The developed neural network based image segmentation can remove unnecessary components of plant images and retain the leaves as the region of interest. The genetic algorithm based committee machine to combine six neural networks with 12 statistical RGB color features as predictors can be used to estimate nitrogen content in wheat leaves more accurately than by using simple averaged neural networks, as well as the SPAD meter and greenness index based methods from previous related works.

REFERENCES

[1] R. Maheswari, K. R. Ashok, and M. Prahadeeswaran, "Precision farming technology, adoption decisions and productivity of vegetables in resource-poor environments," *Agricultural Economics Research Review*, vol. 21, pp. 415-424, 2008.

[2] P. Auearunyawat, T. Kasetkaem, A. Wongmaneeroj, A. Nishihara, and R. Keinprasit, "An automatic nitrogen estimation method in sugarcane

leaves using image processing techniques," *Proc. of Int. Conf. on Agric., Environ. and Biological Sci.* (ICAEBS), 2012, pp. 39–42.

[3] X. Yao, W. Du, S. Feng, and J. Zou, "Image-based plant nutrient status analysis: an overview," *Proc. of IEEE Int. Conf. on Intell. Comput. and Intell. Syst. (ICIS)*, pp. 2492–2495, 2010.

[4] G. Xu, F. Zhang, S. G. Shah, Y. Ye, and H. Mao, "Use of leaf color images to identify nitrogen and potassium deficient tomatoes," *Pattern Recognit. Lett.*, vol. 32, pp. 1584–1590, 2011.

[5] M. A. Hairuddin, N. M. Tahir, and S. R. S. Baki, "Representation of elaeisguineensis nutrition deficiency based on image processing approach," *Proc. of IEEE Int. Conf. on Comput. Appl. and Ind. Electron. (ICCAIE)*, pp. 607–611, 2011.

[6] X. Yuanfang, W. Xianmin, S. Hong, W. Haihua, and Z. Yan'e, "Study of monitoring maize leaf nutrition based on image processing and spectral analysis," *Proc. of IEEE World Autom. Congress (WAC)*, pp. 465–468, 2010.

[7] X. Yao, W. Luo, and Z. Yuan, "An adaptive and quantitative rubber nutrient status analyzing system by digital foliar images," *Proc. of IEEE Int. Congress on Image and Signal Process. (CISP)*, pp. 2492–2495, 2010.

[8] S. Buhan and I. Cadirci, "Multi-stage wind-electric power forecast by using a combination of advanced statistical methods," *IEEE Trans. Ind. Informat*., vol. 11, no. 5, pp.1231–1242, Oct. 2015.

[9] K.Y. Chan, S. Khadem, T.S. Dillon, V. Palade, J. Singh, and E. Chang, "Selection of significant on-road sensor data for short-term traffic flow forecasting using the taguchi method," *IEEE Trans. Ind. Informat*., vol. 8, no. 2, pp. 255-266, May 2012.

[10] M.L. Corradini, V. Fossi, A. Giantomassi, G. Ippoliti, S. Longhi, and G. Orlando, "Minimal resource allocating networks for discrete time sliding mode control of robotic manipulators," *IEEE Trans. Ind. Informat*., vol. 8, no. 4, pp. 733-745, Nov 2012.

[11] Shi-Lu Dai, Cong Wang, and Fei Luo, "Identification and learning control of ocean surface ship using neural networks," *IEEE Trans. Ind. Informat*., vol. 8, no. 4, pp. 801-810, Nov 2012.

[12] C. Wei, W.L. Woo and S.S. Dlay, "Nonlinear underdetermined blind signal separation using Bayesian neural network approach", *Digital Signal Processing*, vol. 17, no. 1, pp. 50-68, 2007.

[13] W.L. Woo and S.S. Dlay, "Neural network approach to blind signal separation of mono-nonlinearly mixed signals", *IEEE Trans. on Circuits and Syst. I*, vol. 52, no. 2, pp. 1236-1247, June 2005.

[14] M. Qasim and V. Khadkikar, "Application of artificial neural networks for shunt active power filter control," *IEEE Trans. Ind. Informat*., vol. 10, no. 3, pp. 1765-1774, Aug. 2014.

[15] W.L. Woo and S.S. Dlay, "Regularised nonlinear blind signal separation using sparsely connected tetwork," *IEE Proc. on Vision, Image and Signal Processing*, vol. 152, no. 1, pp. 61-73, February 2005.

[16] H. D. Cheng, X. Cai, and R. Min, "A novel approach to color normalization using neural network," *Neural Comput. & Applic*., vol. 18, pp. 237–247, 2009.

[17] A. Gijsenij, T. Gevers, and J. van de Weijer, "Computational color constancy: survey and experiments," *IEEE Trans. Image Process*., vol. 20, no. 9, pp. 2475–2489, 2011.

[18] S. Bianco, G. Ciocca, C. Cusano, and R. Schettini, "Improving color constancy using indoor–outdoor image classification," *IEEE Trans. Image Process*., vol. 17, no. 12, pp. 2381–2392, 2008.

[19] K. Barnard, V. Cardei, and B. Funt, "A comparison of computational color constancy algorithms–part I: methodology and experiments with synthesized data," *IEEE Trans. Image Process*., vol. 11, no. 9, pp. 972–983, 2002.

[20] M. Cococcioni, B. Lazzerini, and S.L. Volpi, "Robust diagnosis of rolling element bearings based on classification techniques," *IEEE Trans. Image Process*., vol. 9, no. 4, pp. 2256-2263, Nov. 2013.

[21] Zheng Yan and Jun Wang, "Model predictive control of nonlinear systems with unmodeled dynamics based on feedforward and recurrent neural networks," *IEEE Trans. Image Process*., vol. 8, no. 4, pp. 746-756, Nov 2012.

[22] Ward System Group, "NeuroShell 2," 1998, http://www.wardsystems.com/manuals/neuroshell2/index.html?idxtutorialone.htm.

[23] Q. Zhou, P. Shi, S. Xu, and H. Li, "Observer-based adaptive neural network control for nonlinear stochastic systems with time delay," *IEEE Trans. Neural Netw. Learn. Syst.*, vol. 24, no. 1, pp. 71-80, Jan 2013.

[24] Q. Zhou, P. Shi, Y. Tian, and M. Wang, "Approximation-based adaptive tracking control for MIMO nonlinear systems with input saturation," *IEEE Trans. Cybern.*, vol. 45, no. 10, pp. 2119-2128, Oct 2015.

[25] Changsong Chen and Shanxu Duan, "Optimal integration of plug-in hybrid electric vehicles in microgrids," *IEEE Trans. Ind. Informat*., vol. 10, no. 3, pp. 1917-1926, Aug. 2014.

[26] H. Sung-Ho, K. Reza, and T. Andrew, "Modeling and control of a plastic film manufacturing web process," *IEEE Trans. Ind. Informat*., vol. 7, no. 2, pp. 171–178, May 2011.

[27] R. Vincent, T. Mohammed, and L. Gilles, "Comparison of parallel genetic algorithm and particle swarm optimization for real-time UAV path planning," *IEEE Trans. Ind. Informat*., vol. 9, no. 1, pp. 132–141, Feb. 2013.

[28] P. Charalambos, K. Eftichios, S. Vasilis, K. Tamas, S, Dezso, and T. Remus, "Optimal design of photovoltaic systems using high time-resolution meteorological data," *IEEE Trans. Ind. Informat*., vol. 10, no. 4, pp. 2270–2279, Nov. 2014.

[29] M. Qing-Kui, Z. Chun-Hou, W. Xiao-Feng, L. Feng-Yan, "Recognition of plant leaves using support vector machine," in *Advanced Intelligent Computing Theories and Applications*, vol. 15, Springer-Verlag Berlin Heidelberg, 2008.

[30] C. M. Bishop, Neural Networks for Pattern Recognition, Oxford University Press, 1996.

[31] C. Chen and Z. Lin, "A committee machine with empirical formulas for permeability prediction," *Comput. & Geosci.*, vol. 32, pp. 485–496, 2006.

[32] H. Song, Z. Guo, Y. He, H. Fang, Z. Zhu, "Non-destructive estimation oilseed rape nitrogen status using chlorophyll meter," *Proc. of IEEE Fifth Int. Conf. on Mach. Learning and Cybern*., pp. 4252–4256, 2006.

[33] C. Shengxian, D. Bangkui, S. Jiawei, L. Fan, Y. Shanrang, and X. Zhiming, "A colour constancy algorithm based on neural network and application," *Proc. of IEEE World Congress on Intell. Control and Autom*., pp. 3100–3103, 2010.

[34] X. Xu, X. Zhang, Y. Cai, L. Zhuo, and L. Shen, "Supervised color correction based on QPSO-BP neural network algorithm," *Proc. of IEEE Int. Congress on Image and Signal Process.*, pp. 1–5, 2009.

[35] S. Kawashima and M. Nakatani, "An algorithm for estimating chlorophyll content in leaves using a video camera," *Annals of Botany*, vol. 81, pp. 49–54, 1998.

[36] M. Pagola, R. Ortiz, I. Irigoyen, H. Bustince, E. Barrenechea, P. Aparicio-Tejo, C. Lamsfus, and B. Lasa, "New method to assess barley nitrogen nutrition status based on image colour analysis comparison with SPAD-502", *Computers And Electronics In Agriculture*, vol. 65, pp. 213–218, 2009.

[37] P. Gao, W.L. Woo and S.S. Dlay, "Nonlinear signal separation for multi-nonlinearity constrained mixing model," *IEEE Trans. on Neural Networks*, vol. 17, no. 3, pp. 796-802, May 2006.

[38] P. Gao, W.L. Woo and S.S. Dlay, "Nonlinear independent component analysis using Series Reversion and Weierstrass Network," *IEE Proc. on Vision, Image and Signal Processing*, vol. 153, no. 2, pp. 115-131, 2006.

[39] P. Gao, W.L. Woo and S.S. Dlay, "Weierstrass approach to blind source separation of multiple nonlinearly mixed signals," *IEE Proc. on Circuits, Devices and Systems*, vol. 153, no. 4, pp. 332-345, August 2006.

[40] W.L. Woo and S.S. Dlay, "Nonlinear blind source separation using a hybrid RBF-FMLP network," *IEE Proc. on Vision, Image and Signal Processing*, vol. 152, no. 2, pp. 173-183, April 2005.